

**US-Japan Workshop and Kyoto University 21st COE
Symposium on “New Approach in Plasma Confinement
Experiment in Helical Systems”**

Kyoto, Japan March 1-4, 2004

Presentations are posted at:

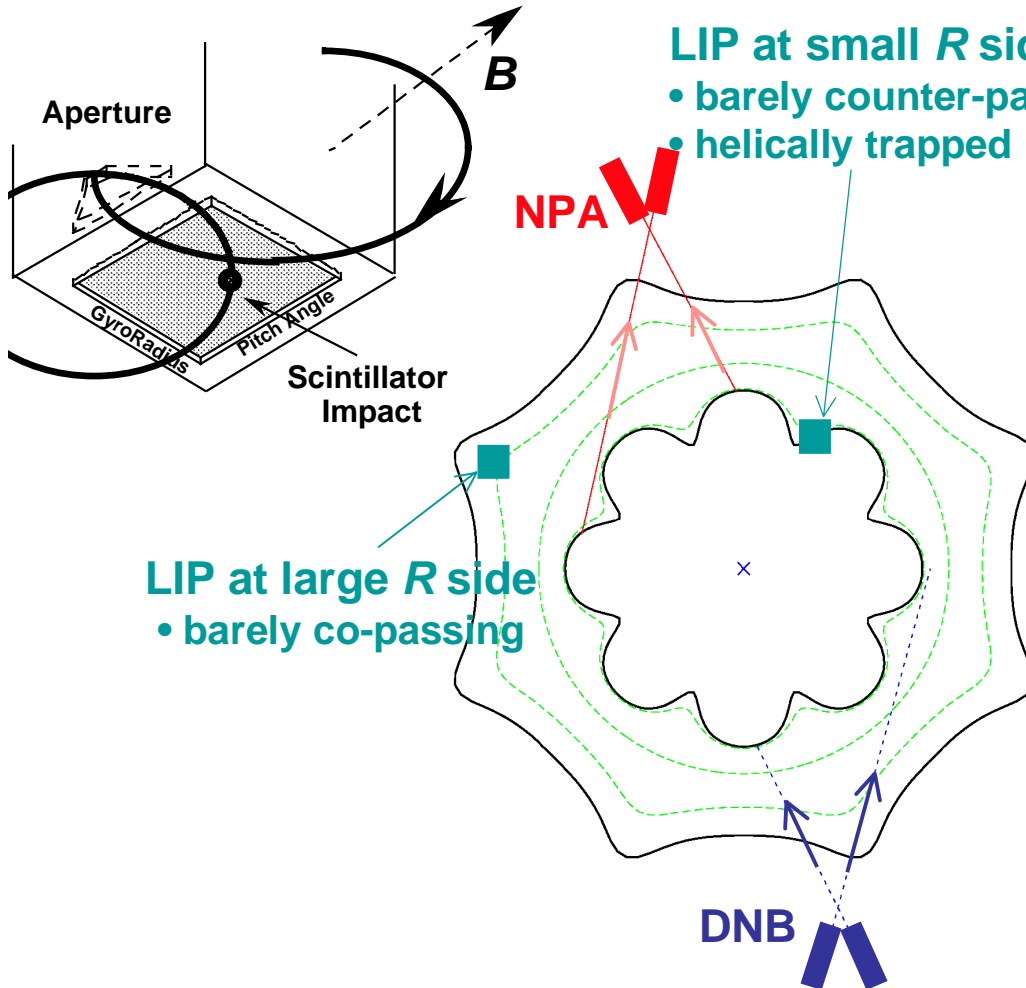
<http://www.center.iae.kyoto-u.ac.jp/plasma/usj04/proceedings.html>

- **Isobe, M., “Experimental study on energetic ion behavior in Compact Helical System(CHS)”**
 - Confinement of tangential NBI
 - Diagnostic neutral beam study of loss cones
 - Enhanced NBI losses from MHD activity
 - ECH driven ion tail formation
- **Murakami, S., “Study of Magnetic Field Optimization Effect on Energetic Particle Confinement in LHD”**
 - Plasma transport and energetic ion confinement in LHD with variable axis shift
 - Different optimizations for thermal transport ($R = 3.53$ m) and energetic ions ($R = 3.6$ m)
 - Alpha losses suppressed in a reactor LHD to $< 2\%$

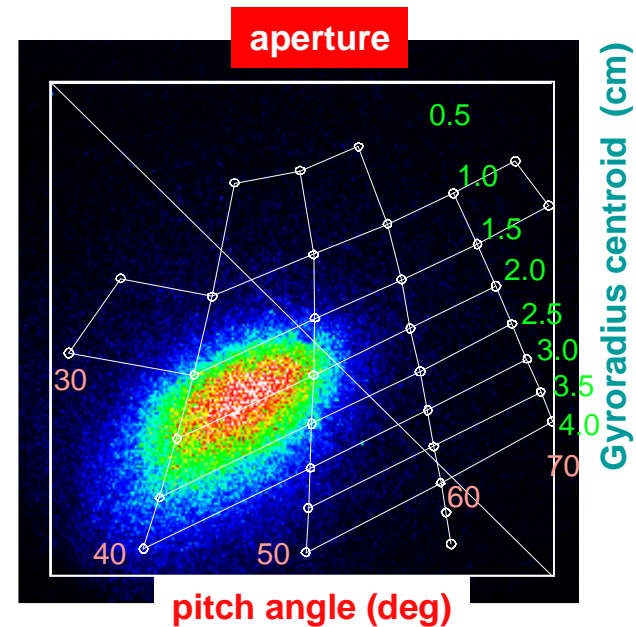
- **Y. Nakamura - “Theoretical Study of the Bootstrap Current in Heliotron J Plasmas”**
 - Uses VMEC2000 + SPBSC (bootstrap model with connection formulas)
 - Finds agreement with Heliotron-J data as inner vertical field current is changed (this varies bumpy component, iota, and vertical elongation)
- **S. Nishimura - “Neoclassical Transport in Advanced Helical Devices”**
 - Momentum conserving corrections to DKES allows calculation of: flows, viscosity, bootstrap current (develops improved connection formulas)
 - Impurity transport -> applied to CHS
- **Y. Suzuki - “Application of 3D MHD Equilibrium codes to Helical system Plasmas”**
 - MHD equilibrium studies/comparisons between VMEC/PIES/HINT
- **B. Blackwell - “Recent Results from the H-1 Heliac”**
 - New method for measuring flux surface quality: visible emission Doppler spectroscopy
 - Configurational effects on particle confinement and MHD fluctuations

Escaping fast ion diagnostic in CHS

- Two lost fast ion probes(LIP) based on a ZnS scintillator are installed in CHS to measure spatial distribution of beam ion loss.
- LIP provides both information of pitch angle and energy of lost fast ions simultaneously.
- LIP is mainly used for study on effect of MHD on fast ion transport.



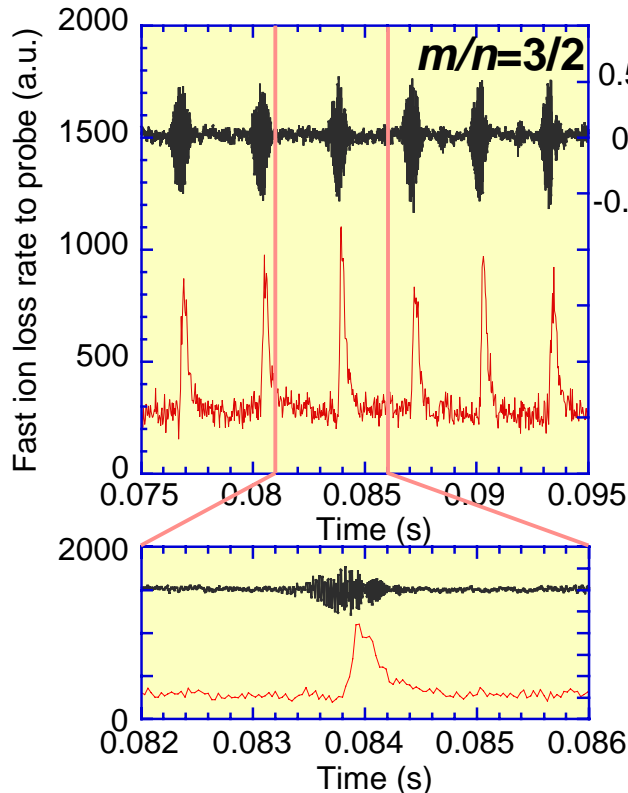
Localized bright spot on the scintillator screen due to impact of lost fast ions



FB type mode enhances beam ion loss to large R side

- In CHS, periodic recurrence of the fishbone(FB) type bursting mode have been observed in co-injected NBI plasmas at B_t of 0.95T.
- Beam ion loss to large R side are periodically enhanced while MHD activities occur and coincides with the timing of fluctuation.

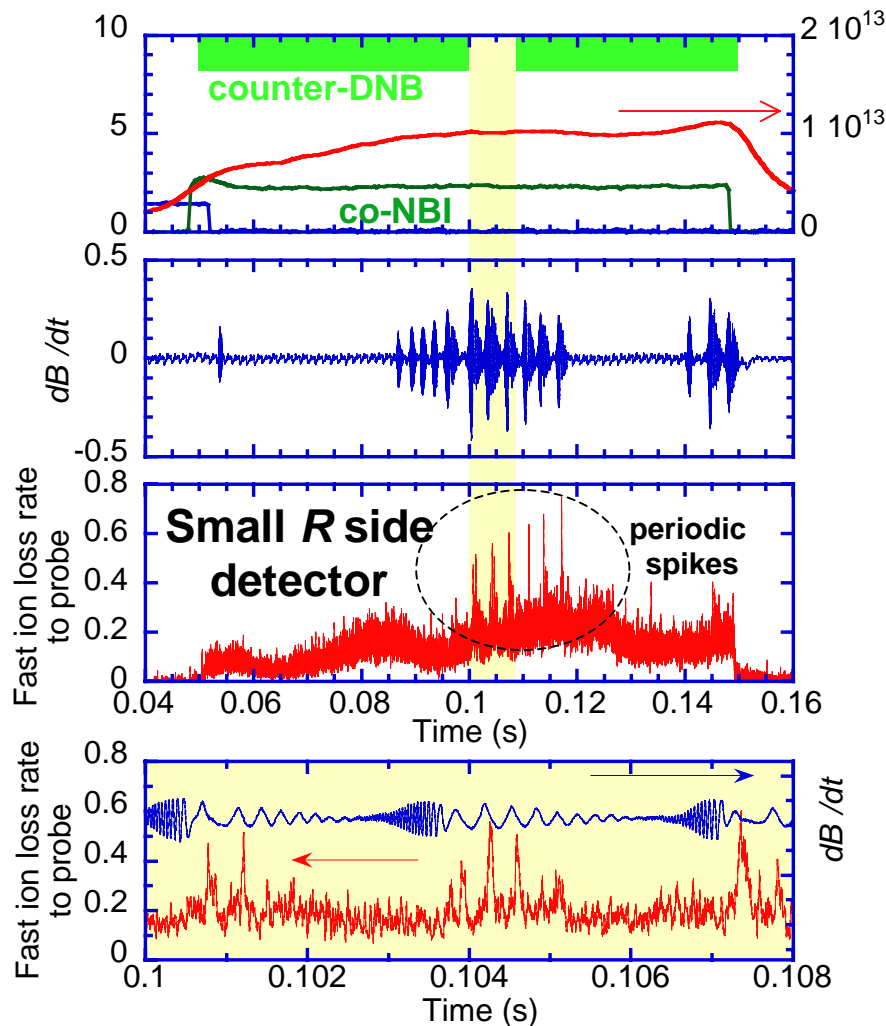
Beam ion loss to large R side detector



- Freq. of the mode is ~ 50 kHz.
- Barely passing beam ions are expelled to large R side and their energy is near E_b (~ 38 keV).
- Enhanced loss of helically trapped ions due to FB mode has never seen at small R side.
- Beam ion loss to large R side does not begin until Mirnov coil reaches a maximum, suggesting mode stabilization after expulsion of beam ions.

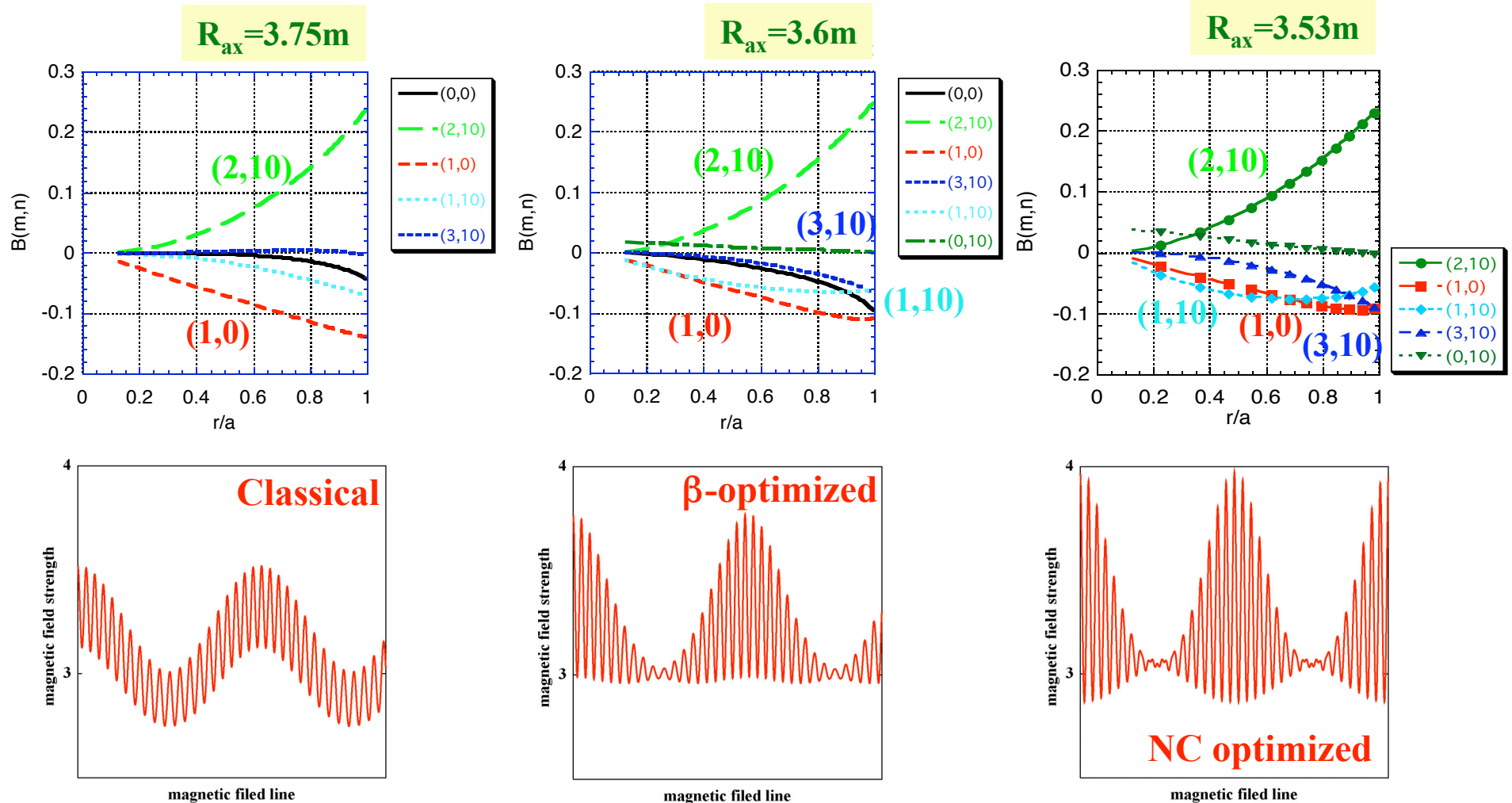
Low freq. mode (~5kHz) enhances loss of counter-going beam ions to small R side

- In order to look into interaction between MHD mode and counter-going beam ions, **DNB is counter- injected into co-injected NBI plasmas.**



- Bursting MHD activities are excited by co-injected heating NB.
- First, high freq. mode (~30-40kHz) appears and then switches to low freq. mode (~3-5kHz).
- Barely counter-passing fast ions are lost in the timing of low freq. mode and their energy is about 10-15keV.
- Expulsion of fast ions to small R side due to high freq. mode is not seen.
- Large R side probe does not detect periodic loss during low freq. mode.

Mod-B Profile of LHD Configurations



- ◆ Inward shift increases the mirror mode $(0,10)$, the sub-harmonic modes; $(1,10)$, $(3,10)$.



S. Murakami et al., Joint Meeting of US-Japan Workshop and Kyoto Univ. 21st COE Symposium, 3 March 2004

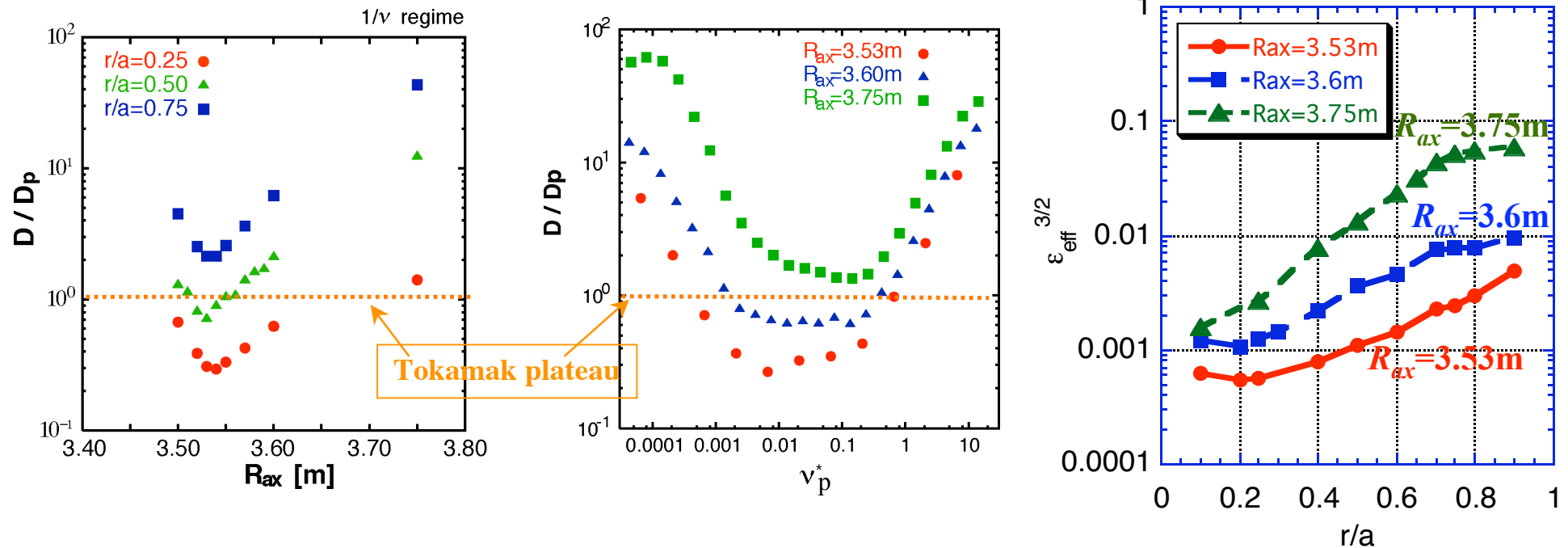


Neoclassical Transport Optimized Configuration

Neoclassical transport analysis (by DCOM)

S. Murakami, et al., Nucl. Fusion 42 (2002) L19.

A. Wakasa, et al., J. Plasma Fusion Res. SERIES, Vol. 4, (2001) 408.



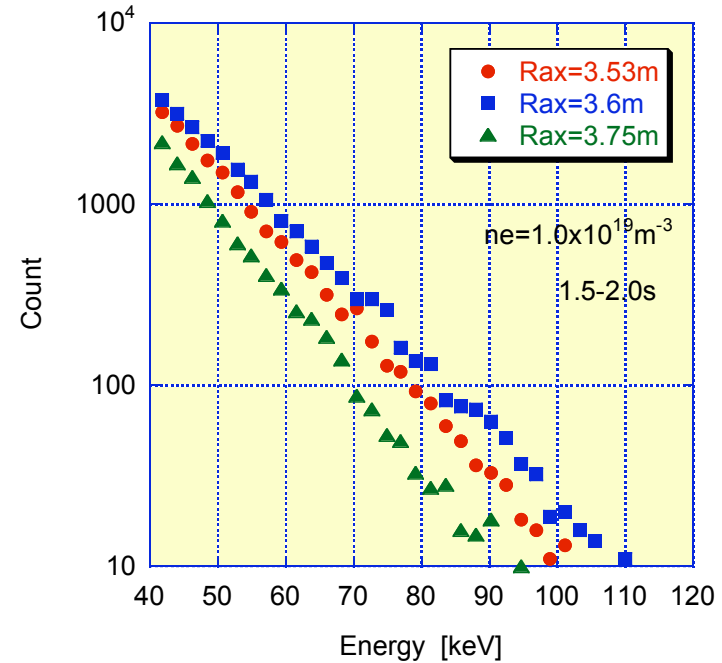
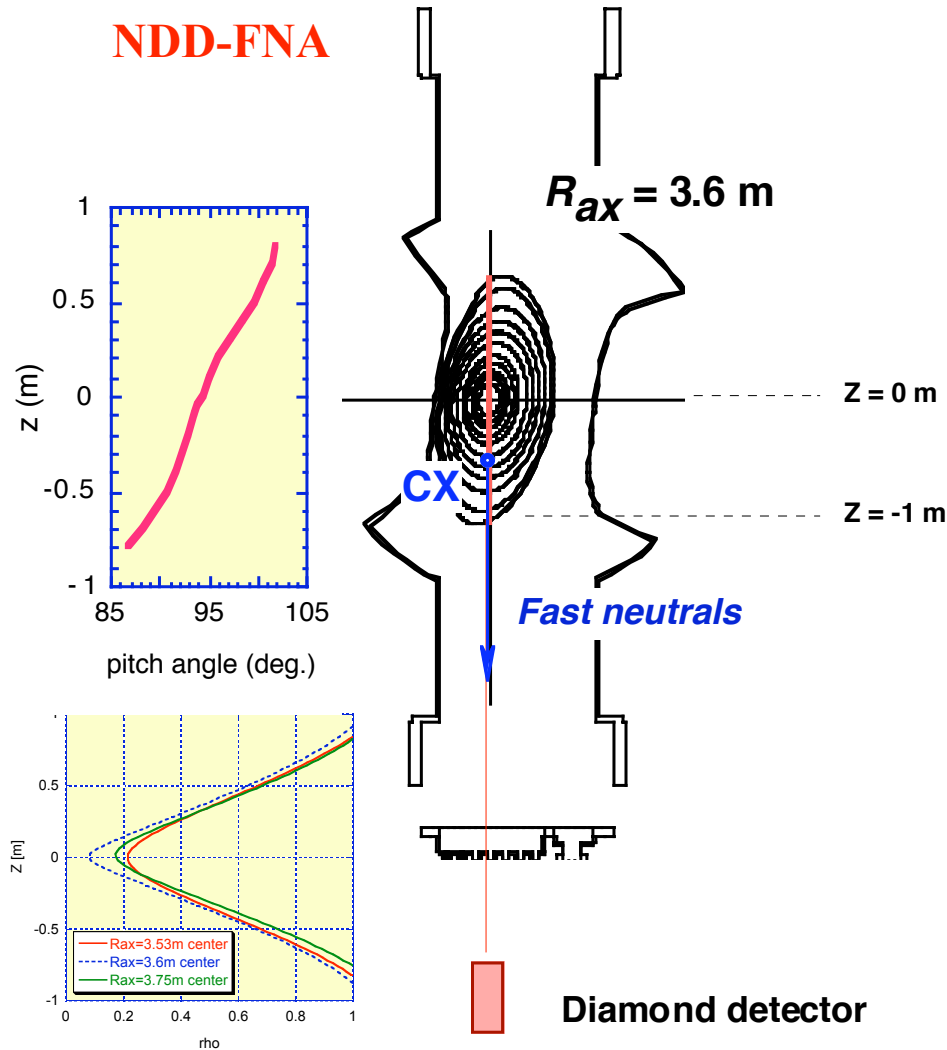
- ◆ We evaluate the neoclassical transport in inward shifted configurations by **DCOM**.
- ◆ The optimum configuration at the $1/\beta$ regime $\Rightarrow R_{ax} = 3.53\text{m}$.
($\beta_{eff} < 2\%$ inside $r/a = 0.8$)
- ◆ A strong inward shift of R_{ax} can diminish the NT to a level typical of so-called "advanced stellarators".



S. Murakami et al., Joint Meeting of US-Japan Workshop and Kyoto Univ. 21st COE Symposium, 3 March 2004



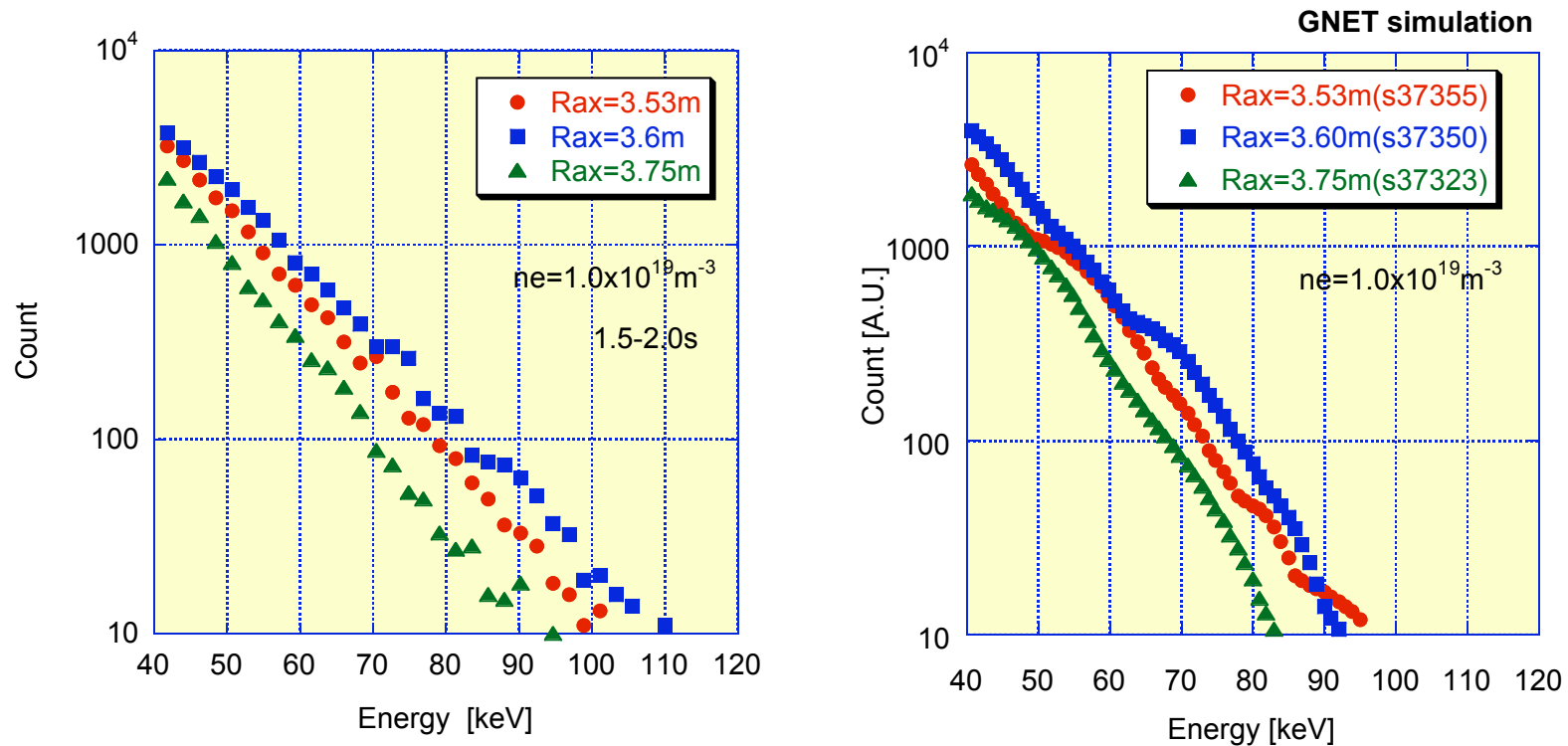
R_{ax} dependency (NDD-FNA)



- ◆ We measured the trapped energetic particle ($v_{||} \sim 0$) by natural diamond detector (NDD)-FNA.
- ◆ Energy spectrums show a linear decrease.

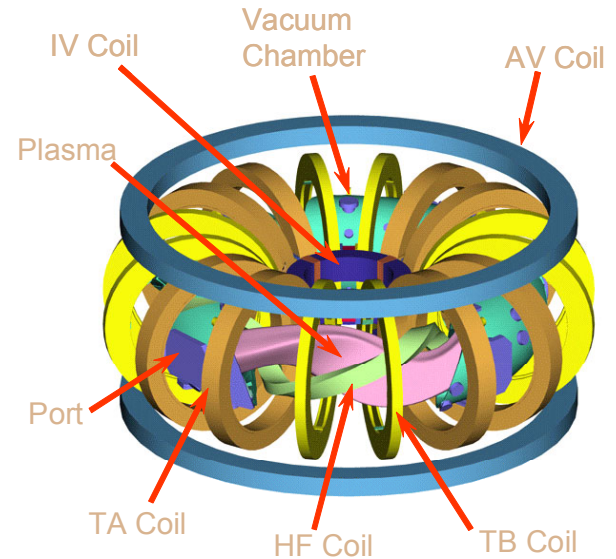
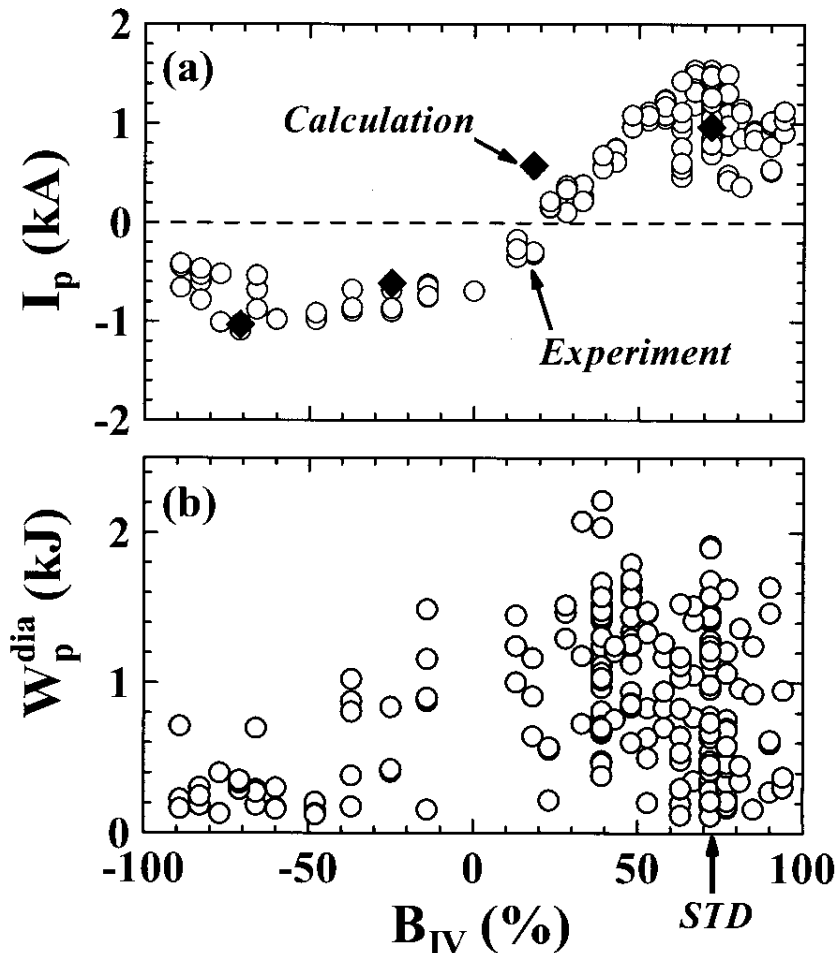
Comparisons with Simulation Results

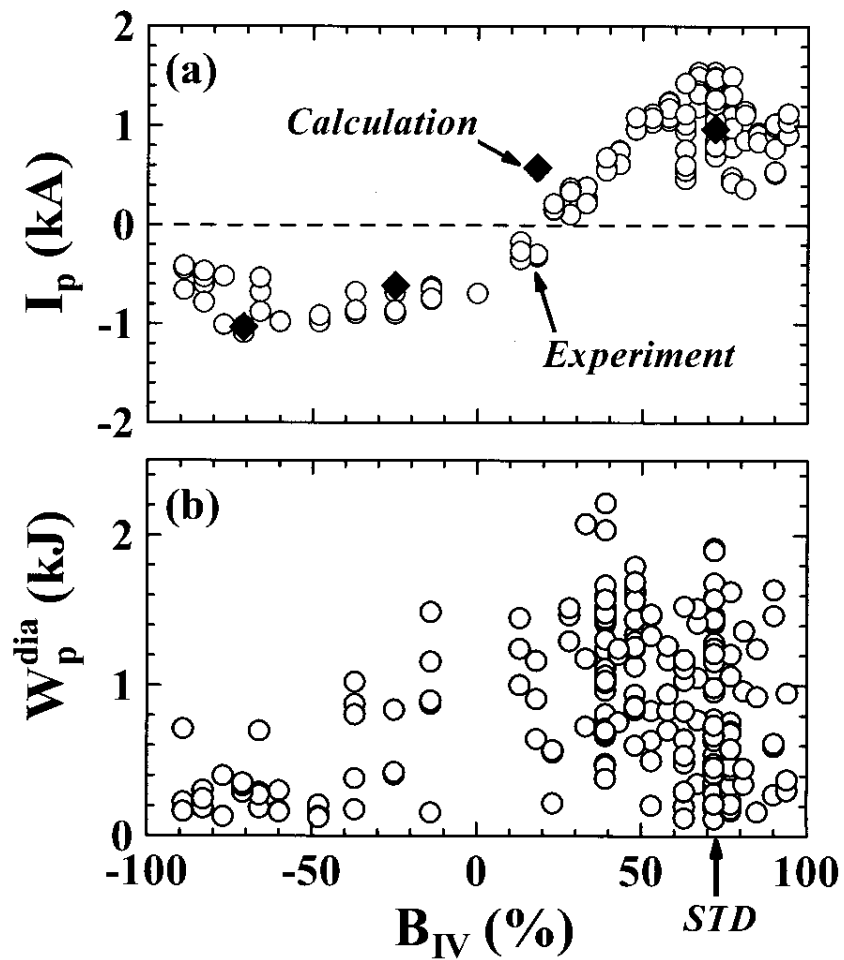
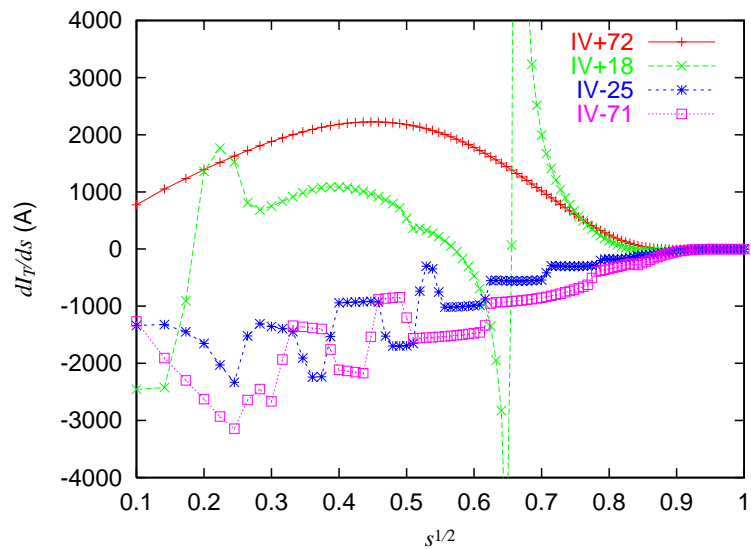
- β The **count rates** are evaluated using a **flux averaged beam ion distribution** by **GNET simulation**.
- β We can see the **similar tendency** of beam ion distributions.



2. Experimental observation of the bootstrap current in Heliotron J

- * Change of the direction of the bootstrap current was observed in H-J experiments when the IV-coil current is varied.

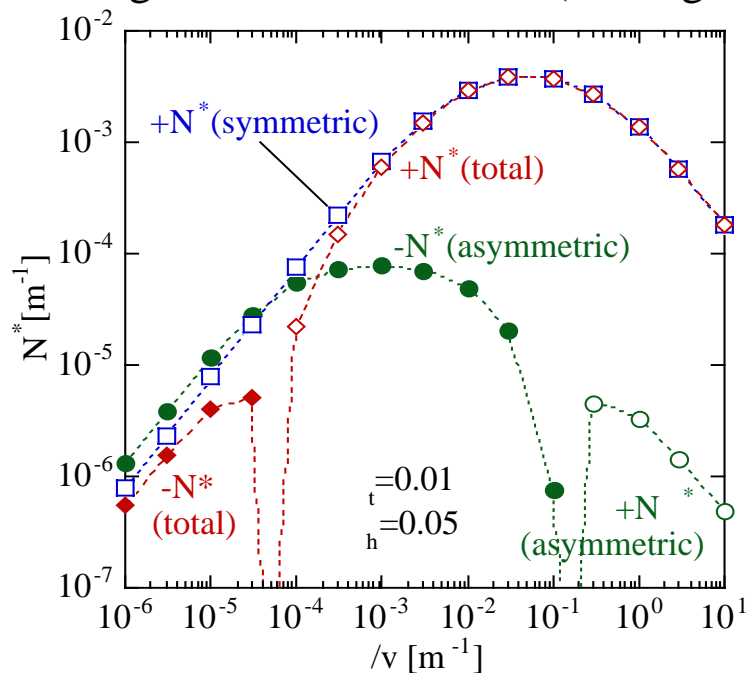




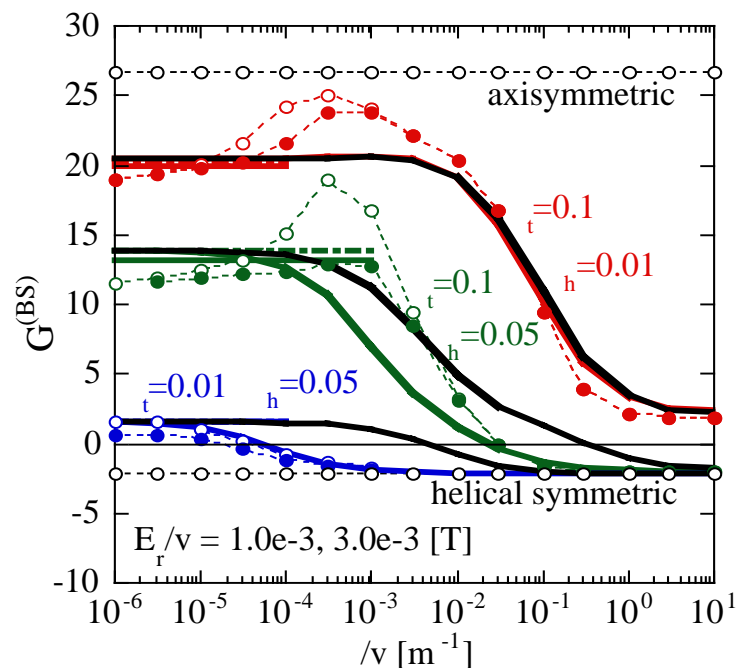
Bootstrap Current Coefficients (3)

(Newly derived connection formula)

Off-diagonal coefficients N^* (driving force)



Geometrical factor $G^{(BS)} \equiv -\langle B^2 \rangle N^*/M^*$



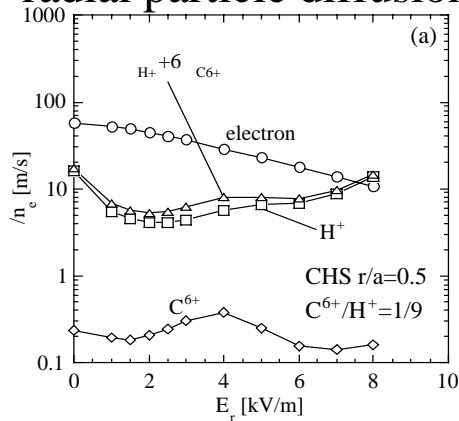
$B = B_0 [1 - \varepsilon_t \cos \theta_B + \varepsilon_h \cos(l\theta_B - n\zeta_B)]$, $l=2$, $n=10$, $B_0=1$ T, $\chi'=0.15$ T•m, $\psi'=0.4$ T•m, $B_\theta=0$, $B_\zeta=4$ T•m are assumed. For various configurations with $0 < \varepsilon_t < 0.1$ and $0 < \varepsilon_h < 0.1$, The analytical expressions for the banana regime derived by Shaing, et al., show good agreements with the numerical results. The effect of the local and global structure, with different field strength variation (δB , ε) and characteristic length (L_c), are well separated.

Diffusions and flows including those of impurity calculation with the parameters in CHS (N-ITB)

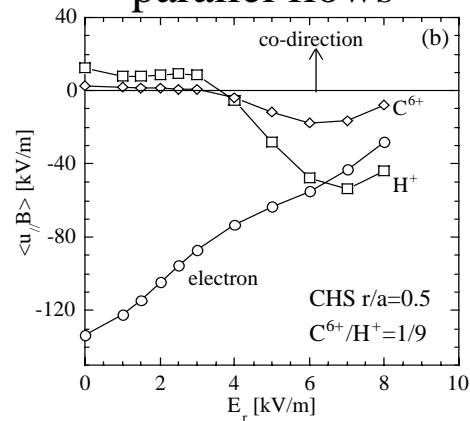
Γ_e^{bn}	=	$L_{e1}^t - L_{ee}^{ee11}$	$L_{e2}^t - L_{ee}^{ee12}$	L_{ea}^{ea11}	L_{ea}^{ea12}	L_{eb}^{eb11}	L_{eb}^{eb12}	L_{1E}^e	A_{e1}
Q_e^{bn}/T_e		$L_{e2}^t - L_{ee}^{ee21}$	$L_{e3}^t - L_{ee}^{ee22}$	L_{ea}^{ea21}	L_{ea}^{ea22}	L_{eb}^{eb21}	L_{eb}^{eb22}	L_{2E}^e	A_{e2}
Γ_a^{bn}		L_{ae}^{ae11}	L_{ae}^{ae12}	$L_{a1}^t - L_{aa}^{aa11}$	$L_{a2}^t - L_{aa}^{aa12}$	L_{ab}^{ab11}	L_{ab}^{ab12}	L_{1E}^a	A_{a1}
Q_a^{bn}/T_a		L_{ae}^{ae21}	L_{ae}^{ae22}	$L_{a2}^t - L_{aa}^{aa21}$	$L_{a3}^t - L_{aa}^{aa22}$	L_{ab}^{ab21}	L_{ab}^{ab22}	L_{2E}^a	A_{a2}
Γ_b^{bn}		L_{be}^{be11}	L_{be}^{be12}	L_{ba}^{ba11}	L_{ba}^{ba12}	$L_{b1}^t - L_{bb}^{bb11}$	$L_{b2}^t - L_{bb}^{bb12}$	L_{1E}^b	A_{b1}
Q_b^{bn}/T_b		L_{be}^{be21}	L_{be}^{be22}	L_{ba}^{ba21}	L_{ba}^{ba22}	$L_{b2}^t - L_{bb}^{bb21}$	$L_{b3}^t - L_{bb}^{bb22}$	L_{2E}^b	A_{b2}
J_E^{BS}		L_{E1}^e	L_{E2}^e	L_{E1}^a	L_{E2}^a	L_{E1}^b	L_{E2}^b	L_{EE}	A_E

$$Q_a^{bn} \equiv q_a^{bn} + (5/2) \Gamma_a^{bn} T_a \quad A_a \equiv \begin{bmatrix} A_{a1} \\ A_{a2} \end{bmatrix} \equiv -T_a \begin{bmatrix} \frac{n_a'}{n_a} - \frac{3}{2} \frac{T_a'}{T_a} - \frac{e_a \phi'}{T_a} \\ T_a'/T_a \end{bmatrix} \quad A_E \equiv \langle BE_{||} \rangle / \langle B^2 \rangle^{1/2}$$

radial particle diffusion



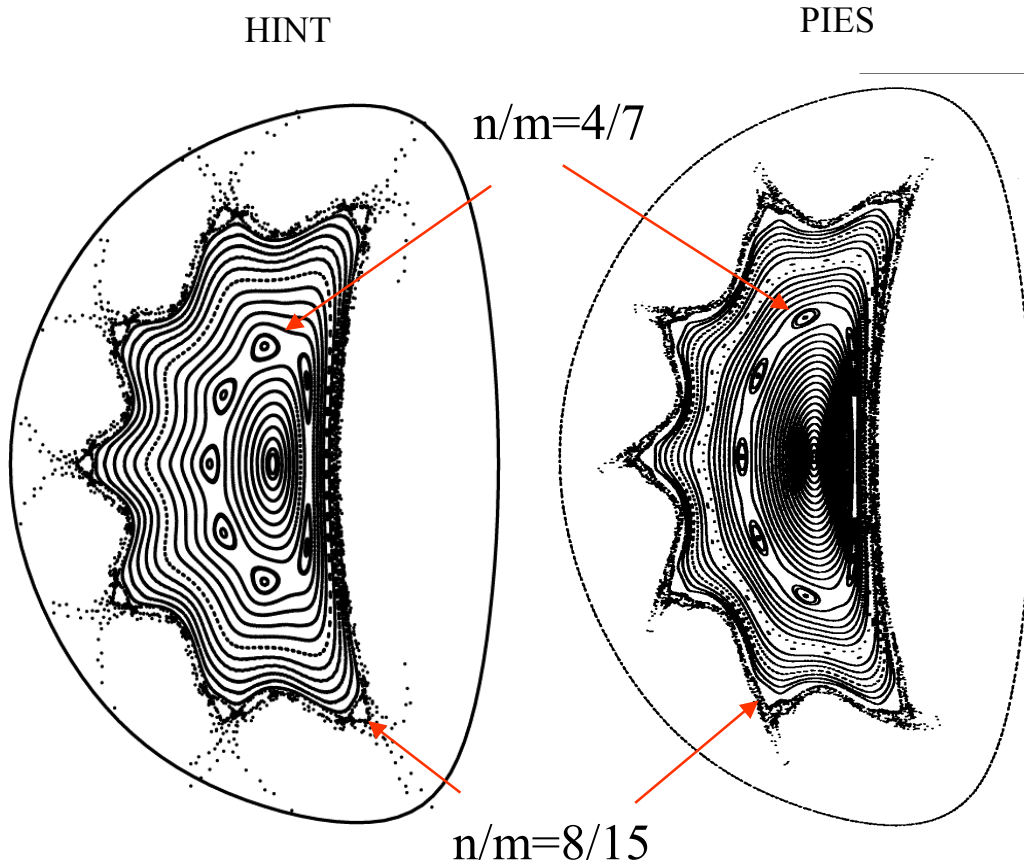
parallel flows



Comparison between HINT and PIES codes

By calculation of HINT and PIES, 'standard configuration' of Heliotron J has magnetic islands for finite beta equilibria ($>0.5\%$).

$$\beta_0 = 1.5\% \quad p = p_0(1-s)^2$$



Both results are similar.

- Resonances 4/7 and 8/15
- Phase

Details are slightly different

- Island width
- Position of resonance 4/7
- Shape of surfaces

Why?

Difference of scheme

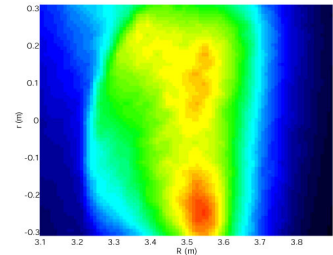
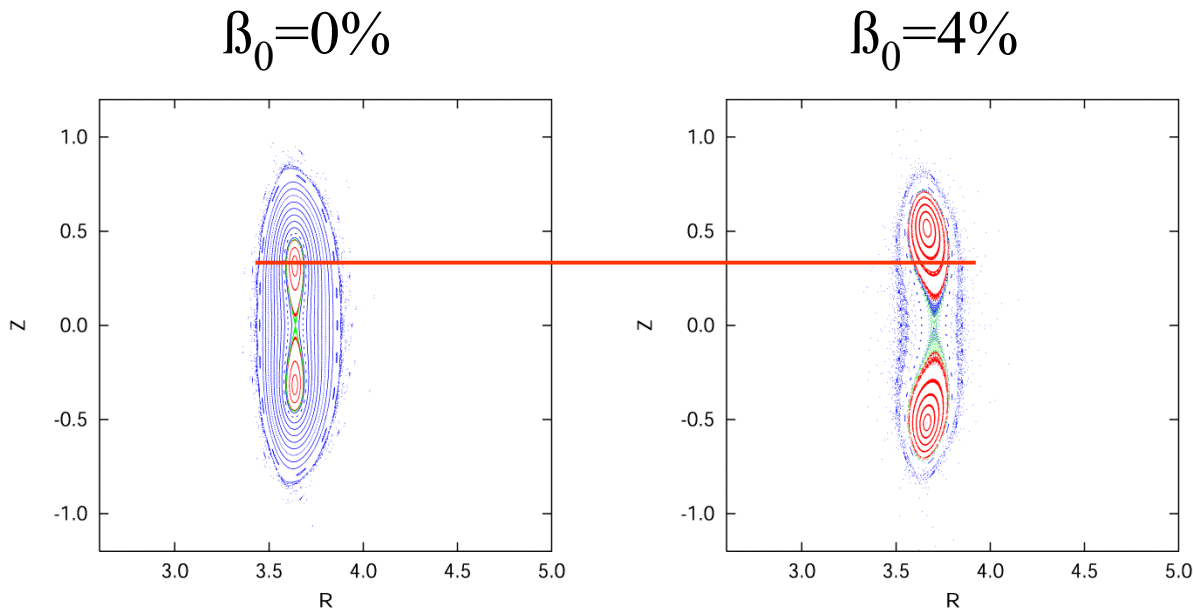
Difference of coordinates



Detailed comparison is required.

Application of HINT code to other configurations

MHD Equilibrium of double axes configuration in LHD (preliminary results)



In the recent LHD experiments, the double axes configuration was produced. (K.Ida *et al.*)

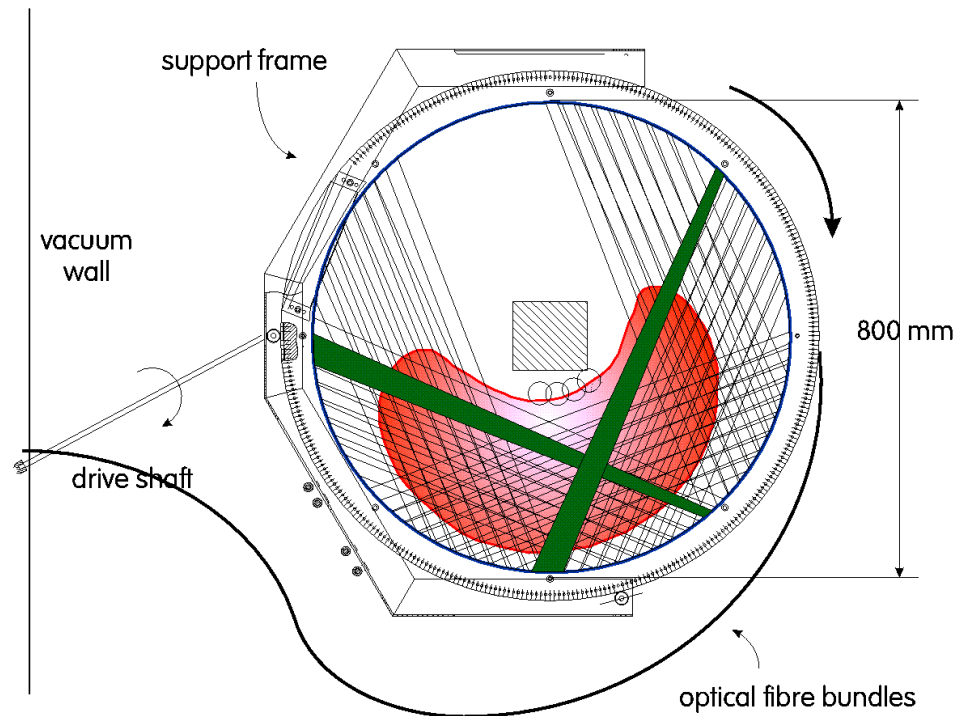
Properties of finite β equilibrium

- horizontal shift is very small but vertical shift from equatorial plane is large.
- X-point inside separatrix slightly moves outside of torus.
- Structure of magnetic field lines outside separatrix is stochastic.

Horizontal elongated configurations are studied in progress.

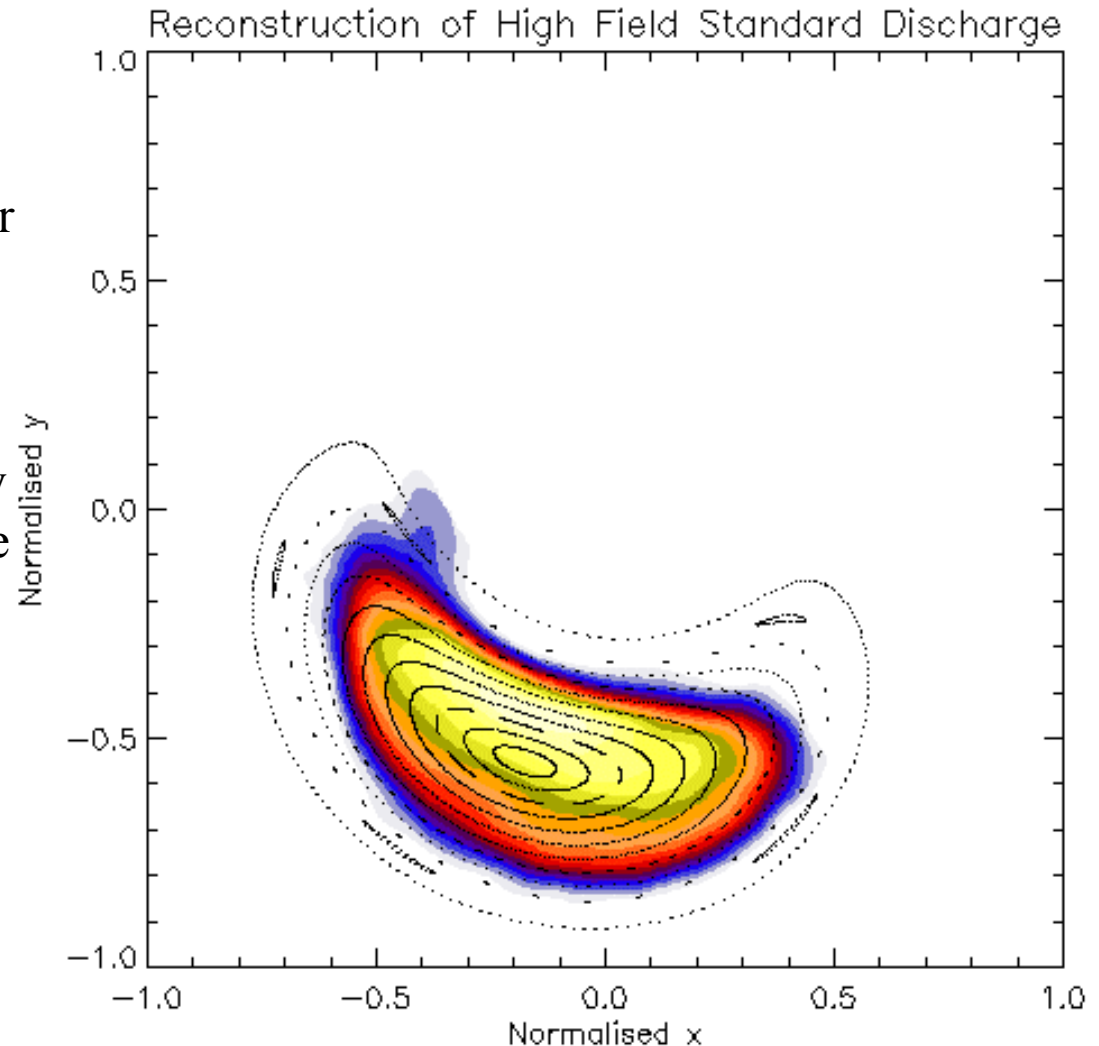
Configuration Mapping in Plasma: Visible Emission Doppler Spectroscopy

- “MOSS” Doppler spectrometer with 55 views → 2D imaging
- Time-resolved inversion from a single shot, with constraints
 - e.g. magnetic surfaces
- Shot averaged inversion with no flux surface assumptions



Standard configuration

- Visible ion emission tomography
- In preparation for Doppler ion tomography
- No assumption of magnetic surfaces
- Ion line emission strongly weighted to plasma centre ($n_i n_e$) – outer surfaces would be better sensed with a neutral line.



Extreme test configuration – $\iota \sim 3/2$

- No assumption of magnetic surfaces
- Proves quality of tomographic data
- Shows that quantitative mapping of surfaces can be performed under plasma conditions

